

CLASSIFICATION WITH INVARIANT SCATTERING REPRESENTATIONS

Joan Bruna and Stéphane Mallat

CMAP, École Polytechnique
Rue de Saclay, Palaiseau, France

ABSTRACT

A scattering transform defines a signal representation which is invariant to translations and Lipschitz continuous relatively to deformations. It is implemented with a non-linear convolution network that iterates over wavelet and modulus operators. Lipschitz continuity locally linearizes deformations. Complex classes of signals and textures can be modeled with low-dimensional affine spaces, computed with a PCA in the scattering domain. Classification is performed with a penalized model selection. State of the art results are obtained for handwritten digit recognition over small training sets, and for texture classification.¹

Index Terms— Image classification, Invariant representations, local image descriptors, pattern recognition, texture classification.

1. INTRODUCTION

Affine space models are simple to compute with a Principal Component Analysis (PCA) but are not appropriate to approximate signal classes that include complex forms of variability. Image classes are often invariant to rigid transformations such as translations or rotations, and include elastic deformations, which define highly non-linear manifolds. Textures may also be realizations of strongly non-Gaussian processes that cannot be discriminated with linear models either.

Kernel methods define distances $d(f, g) = \|\Phi(f) - \Phi(g)\|$, with operators Φ which address these issues by mapping f and g into a space of much higher dimension. However, invariance properties and learning requirements on small training sets, rather suggest to implement a dimensionality reduction.

Scattering operators constructed in [9, 10], are invariant to global translations and Lipschitz continuous relatively to local deformations, up to a log term, thus providing local translation invariance through the linearization of such deformations. These scattering operators create invariance by averaging interference coefficients, which capture signal interactions at several scales and orientations. This paper models complex signal classes with low-dimensional affine spaces in

the scattering domain, which are computed with a PCA. The classification is performed by a penalized model selection.

Scattering operators may also be invariant to any compact Lie subgroup of $GL(\mathbb{R}^2)$, such as rotations, but we concentrate on translation invariance, which carries the main difficulties and already covers a wide range of classification applications. Section 2 reviews the construction of scattering operators with a cascade of wavelet transforms and modulus operators, which defines a non-linear convolution network [6]. Section 3 shows that learning affine scattering model spaces has a linear complexity in the number of training samples. Section 4 describes state of the art classification results obtained from limited number of training samples in the MNIST hand-written digit database, and for texture classification in the CUREt database. Software is available at www.cmap.polytechnique.fr/scattering.

2. SCATTERING OPERATORS

In order to build a representation which is locally translation invariant, a scattering transform begins from a wavelet representation. Translation invariance is obtained by progressively mapping high frequency wavelet coefficients to lower frequencies, with modulus operators described in Section 2.1. Scattering operators, defined in 2.2, iterate over wavelet modulus operators. Section 2.3 shows that it defines a translation invariant representation, which is Lipschitz continuous to deformation, up to a log term.

2.1. Wavelet Modulus Propagator

A wavelet transform extracts information at different scales and orientations by convolving a signal f with dilated band-pass wavelets ψ_γ having a spatial orientation angle $\gamma \in \Gamma$:

$$W_{j,\gamma}f(x) = f \star \psi_{j,\gamma}(x) \text{ with } \psi_{j,\gamma}(x) = 2^{-2j}\psi_\gamma(2^jx).$$

At the largest scale 2^J , low-frequencies are carried by a low-pass scaling function ϕ : $A_Jf = f \star \phi_J$, with $\phi_J(x) = 2^{-2J}\phi(2^{-J}x)$ and $\int \phi(x) dx = 1$. The resulting wavelet representation is

$$\overline{W}_Jf = \{A_Jf, W_{j,\gamma}f\}_{j < J, \gamma \in \Gamma}.$$

¹This work is funded by the ANR grant 0126 01.

The norm of the wavelet operator is defined by

$$\|\overline{W}_J f\|^2 = \|f \star \phi_J\|^2 + \sum_{j < J, \gamma \in \Gamma} \|W_{j,\gamma} f\|^2 \quad (1)$$

with $\|f\|^2 = \int |f(x)|^2 dx$ and it satisfies

$$(1 - \delta)\|f\|^2 \leq \|\overline{W}_J f\|^2 \leq \|f\|^2 \quad (2)$$

if and only if for all $\omega \in \mathbb{R}^2$,

$$1 - \delta \leq |\hat{\phi}(2^J \omega)|^2 + \frac{1}{2} \sum_{j < J, \gamma \in \Gamma} (|\hat{\psi}_\gamma(2^j \omega)|^2 + |\hat{\psi}_\gamma(-2^j \omega)|^2) \leq 1. \quad (3)$$

We consider families of complex wavelets

$$\psi_\gamma(x) = e^{i\xi_\gamma x} \theta_\gamma(x)$$

where $\theta_\gamma(x)$ are low-pass envelopes. Oriented Gabor functions are examples of complex wavelets, obtained with a modulated Gaussian $\psi(x) = e^{i\xi \cdot x} e^{-|x|^2/(2\sigma^2)}$, which is rotated with R_γ by an angle $\pi\gamma/|\Gamma|$: $\psi_\gamma(x) = \psi(R_\gamma x)$. In numerical experiments, we set $\xi = 3\pi/4$, $\sigma = 1$, $|\Gamma| = 6$, and ϕ is also a Gaussian with $\sigma = 2/3$. It satisfies (3) only over a finite range of scales.

If $f_\tau(x) = f(x - \tau)$ then

$$W_{j,\gamma} f_\tau(x) = W_{j,\gamma} f(x - \tau) \approx W_{j,\gamma} f(x)$$

if and only if $|\tau| \ll 2^j$, because $W_{j,\gamma} f$ has derivatives of amplitude proportional to 2^{-j} . High frequencies corresponding to fine scales are thus highly sensitive to translations.

Translation invariance is improved by mapping high frequencies to lower frequencies with a complex modulus operator. Since $\psi_\gamma(x) = e^{i\xi_\gamma x} \theta_\gamma(x)$, we verify that

$$W_{j,\gamma} f(x) = e^{i\xi_{j,\gamma} x} (f_{j,\gamma} \star \theta_{j,\gamma}(x)),$$

where $\xi_{j,\gamma} = 2^{-j}\xi_\gamma$, $\theta_{j,\gamma}(x) = 2^{-2j}\theta_\gamma(2^{-j}x)$ and $f_{j,\gamma}(x) = e^{i\xi_{j,\gamma} x} f(x)$. Wavelet coefficients $W_{j,\gamma} f(x)$ are located at high frequencies because of the $e^{i\xi_{j,\gamma} x}$ term. These oscillations are removed by a modulus operator

$$|W_{j,\gamma} f| = |f_{j,\gamma} \star \theta_{j,\gamma}(x)|. \quad (4)$$

The energy of $|W_{j,\gamma} f|$ is now mostly concentrated in the low frequency domain covered by the envelop $\hat{\theta}_{j,\gamma}(\omega) = \hat{\theta}_\gamma(2^j \omega)$. It may however also include some high frequencies produced by the modulus singularities where $f_{j,\gamma} \star \theta_{j,\gamma}(x) = 0$. Using complex wavelets is important to reduce the number of such singularities and thus concentrate the information at low frequencies.

If $f(x) = \sum_n a_n \cos(\omega_n x)$ then one can verify that $|W_{j,\gamma} f(x)| = c_{j,\gamma} + \epsilon_{j,\gamma}(x)$ where $\epsilon_{j,\gamma}(x)$ is an interference term. It is a combination of the $\cos(\omega_n - \omega_{n'})x$, for all ω_n and $\omega_{n'}$ in the support of $\hat{\psi}_\gamma(2^j \omega)$. The modulus yields interferences that depend upon frequency intervals, but it loses the exact frequency locations ω_n in each octave.

A wavelet modulus propagator is obtained by applying a complex modulus to all wavelet coefficients:

$$\overline{U}_J f = \{A_J f, |W_{j,\gamma} f|\}_{j < J, \gamma \in \Gamma}.$$

Since $\|a\| - \|b\| \leq \|a - b\|$ and the wavelet transform is contractive, it results that

$$\|\overline{U}_J f - \overline{U}_J g\| \leq \|\overline{W}_J f - \overline{W}_J g\| \leq \|f - g\|$$

and $\|\overline{U}_J f\| = \|f\|$ if $\delta = 0$ in (2).

2.2. Multiple Paths Scattering

Thanks to the concentration towards the low frequencies, the interference coefficients of the wavelet modulus propagator can be locally averaged by ϕ_J in order to produce locally translation invariant coefficients with non negligible energy:

$$|f \star \psi_{j_1, \gamma_1}| \star \phi_J(x).$$

The high frequencies of $|f \star \psi_{j_1, \gamma_1}|$ not removed by the convolution with ϕ_J are carried by the wavelet coefficients $|f \star \psi_{j_1, \gamma_1}| \star \psi_{j_2, \gamma_2}$ at scales $2^{j_2} < 2^{j_1}$. To become insensitive to local translation and reduce the variability of these coefficients, their complex phase can also be removed by a modulus which is also averaged by ϕ_J :

$$||f \star \psi_{j_1, \gamma_1}| \star \psi_{j_2, \gamma_2}| \star \phi_J.$$

These second order coefficients provide co-occurrence information at two scales 2^{j_1} , 2^{j_2} and in two directions γ_1 and γ_2 . This can distinguish corners and junctions from edges and characterize texture structures. Coefficients are only calculated for $2^{j_2} < 2^{j_1}$ because one can show [10] that if ψ is an appropriate complex wavelet then $|f \star \psi_{j_1, \gamma_1}| \star \psi_{j_2, \gamma_2}$ is negligible at scales $2^{j_2} \geq 2^{j_1}$.

The high frequencies lost by the filtering with ϕ_J can again be restored with finer scale wavelet coefficients, which are regularized by suppressing their phase with a modulus and by averaging the result with ϕ_J . Applying iteratively this procedure n times yields the following coefficients:

$$|||f \star \psi_{j_1, \gamma_1}| \star \psi_{j_2, \gamma_2}| \dots \star \psi_{j_n, \gamma_n}| \star \phi_J(x).$$

At any location x , they provide co-occurrence information between any of the $|\Gamma|^n$ families of angles $1 \leq \gamma_1, \dots, \gamma_n \leq |\Gamma|$ and any of the $\binom{J}{n}$ families of scales satisfying $0 \leq j_1 < \dots < j_n < J$. They are called scattering coefficients because they can be interpreted as interaction coefficients between f and the successive wavelets $\psi_{j_1, \gamma_1} \dots \psi_{j_n, \gamma_n}$.

A scattering operator considers all the scattering coefficients at all scales and orientations up to a maximum co-occurrence order m . It is indexed along a path variable $p = \{(j_n, \gamma_n)\}_{n \leq |p| \leq m}$ which is a family of wavelet indices. It

computes $|p|$ wavelet convolutions and modulus along the path

$$S_J(p)f = \underbrace{|\cdots|}_{|p|} f \star \psi_{j_1, \gamma_1} \star \psi_{j_2, \gamma_2} \cdots \star \psi_{j_{|p|}, \gamma_{|p|}} \star \phi_J$$

with $j_n < J$ and $\gamma_n \in \Gamma$. Its dimension is $\sum_{n=0}^m |\Gamma|^n \binom{J}{n}$.

One can verify that scattering coefficients for paths of length m' are computed by applying the wavelet modulus propagator \bar{U}_J to scattering coefficients for all paths p of length $|p| = m' - 1$:

$$\{\bar{U}_J S(p)f\}_{p, |p|=m'-1} = \{S_J(p)f\}_{p, |p|=m'-1} \cup \{S(p)f\}_{p, |p|=m'} \quad (5)$$

where $S(p)f = \underbrace{|\cdots|}_{|p|} f \star \psi_{j_1, \gamma_1} \star \psi_{j_2, \gamma_2} \cdots \star \psi_{j_{|p|}, \gamma_{|p|}} \star \phi_J$.

A scattering operator is thus computed with a cascade of convolutions and modulus operators over $m+1$ layers, similar to the convolution network architecture introduced by LeCun [6, 3]:

$$\begin{array}{ccc} f & \rightarrow & \boxed{f \star \phi_J} \\ \downarrow & & \\ |f \star \psi_{j_1, \gamma_1}| & \rightarrow & \boxed{|f \star \psi_{j_1, \gamma_1}| \star \phi_J} \\ \downarrow & & \\ ||f \star \psi_{j_1, \gamma_1} \star \psi_{j_2, \gamma_2}| & \rightarrow & \boxed{||f \star \psi_{j_1, \gamma_1} \star \psi_{j_2, \gamma_2}| \star \phi_J} \\ \downarrow & & \\ \dots & & \end{array}$$

After convolution with ϕ_J the output can be subsampled at intervals 2^J . If f is an image of N pixels, this uniform sampling yields a scattering representation $S_J f$ including a total of $N_J = 2^{-2J} N \sum_{n=0}^m |\Gamma|^n \binom{J}{n}$ coefficients. The output of any wavelet convolution and modulus $|\dots \star \psi_{j,k}|$ can be subsampled at intervals 2^{j-1} which reduces intermediate computations and barely introduces any aliasing. With an FFT, the overall computational complexity is then $O(N \log N)$.

2.3. Scattering Metric and Deformation Stability

For appropriate complex wavelets, one can prove [10] that the energy $\sum_{|p|=m} \|S_J(p)f\|^2$ of a scattering layer m tends to zero as m increases. This decay is fast. Numerically the maximum network depth is typically limited to $m_0 = 3$.

The scattering metric is obtained with a summation over all paths p :

$$\|S_J f - S_J g\|^2 = \sum_p \|S_J(p)f - S_J(p)g\|^2,$$

where $\|S_J(p)f\|^2 = \int |S_J(p)f(x)|^2 dx$. Since S_J is calculated by iterating on the contractive propagator \bar{U}_J (5), it results that it is also contractive [8]

$$\|S_J f - S_J g\|^2 \leq \|f - g\|^2.$$

Scattering operators are not only contractive but also preserve the norm. For appropriate complex wavelets which satisfy (3) for $\delta = 0$, one can prove [10] that $\|S_J f\| = \|f\|$.

When a signal is translated $f_\tau(x) = f(x - \tau)$, the scattering transform is also translated

$$S_J(p)f_\tau(x) = S_J(p)f(x - \tau)$$

because it is computed with convolutions and modulus. However, when J increases, $S_J(p)f(x)$ tends to a constant because of the convolutions with ϕ_J . It thus becomes translation invariant and one can verify [10] that the asymptotic scattering metric is translation invariant:

$$\lim_{J \rightarrow \infty} \|S_J f - S_J f_\tau\| = 0.$$

For classification the key scattering property is its Lipschitz continuity to deformations $D_\tau f(x) = f(x - \tau(x))$. Let $|\tau|_\infty = \sup_x |\tau(x)|$ and $|\nabla \tau|_\infty = \sup_x |\nabla \tau(x)| < 1$, where $|\nabla \tau(x)|$ is the matrix sup norm of $\nabla \tau(x)$. Along paths of length $|p| \leq m_0$, one can prove [10] that for all $2^J \geq |\tau|_\infty / |\nabla \tau|_\infty$ the scattering metric satisfies

$$\|S_J D_\tau f - S_J f\| \leq C m_0 \|f\| |\nabla \tau|_\infty \log \frac{|\tau|_\infty}{|\nabla \tau|_\infty}. \quad (6)$$

The scattering operator is thus Lipschitz continuous to deformations, up to a log term. It shows that for sufficiently large scales 2^J , the signal translations and deformations are locally linearized by the scattering operator.

3. CLASSIFICATION

Local translation invariance and Lipschitz regularity to local deformations linearize small deformations. Signal classes can thus be approximated with low-dimensional affine spaces in the scattering domain. Although the scattering representation is implemented with a potentially deep convolution network, learning is not deep and it is reduced to PCA computations. The classification is implemented with a penalized model selection.

3.1. Affine Scattering Space Models

A signal class \mathcal{C} can be modeled as a realization of a random process F . There are multiple sources of variability, due to the reflectivity of the material as in textures, due to deformations or to various illuminations. Illumination variability is often low-frequency and can be approximated in linear spaces of dimension close to 10 [1]. This property remains valid in the scattering domain. A scattering operator also linearizes local deformations and reduces the variance of large classes of stationary processes. One can thus build a linear affine space approximation of $S_J F$. A scattering transform $S_J F$ along progressive paths of length $|p| \leq m_0$ is a vector of size $O(N)$, which may be much smaller than N if J is large.

The affine space \mathbf{A}_k of dimension k which minimizes the expected projection error $E\{\|S_J F - P_{\mathbf{A}_k}(S_J F)\|^2\}$ is

$$\mathbf{A}_k = \mu_J + \mathbf{V}_k \quad (7)$$

where $\mu_J(p, x) = E\{S_J(p)F(x)\}$ and \mathbf{V}_k is the space generated by the first k eigenvectors of the covariance operator of $S_J(p)F(x)$. The space dimension k is limited to a maximum value K .

These affine space models are estimated by computing the empirical average and the empirical covariance of $S_J(p)f(x)$, for all training signals $f \in \mathcal{C}$. The empirical covariance is diagonalized to estimate the K eigenvectors of largest eigenvalues. Under mild conditions [14], the sample covariance matrix $\hat{\Sigma}$ converges in norm to the true covariance when the number of training signals is of the order of the dimensionality of the space where $S_J F$ belongs. Dimensionality reduction is thus important to learn affine space models from few training signals.

The computational complexity to estimate affine space models $\hat{\mathbf{A}}_k$ is dominated by eigenvectors calculations. To compute the first K eigenvectors, a thin SVD algorithm requires $O(T K N)$ operations, where T is the number of training signals.

3.2. Linear Model Selection

Let us consider a classification problem with several classes $\{\mathcal{C}_i\}_{1 \leq i \leq I}$. We introduce a classification algorithm which selects affine space models by minimizing a penalized approximation error.

Each class \mathcal{C}_i is represented by a family of embedded affine spaces $\mathbf{A}_{k,i} = \hat{\mu}_i + \mathbf{V}_{k,i}$, where $\mathbf{V}_{k,i}$ is the space generated by the first k eigenvectors $\{e_{i,l}\}_{l \leq k}$ of the empirical covariance matrix $\hat{\Sigma}_i$. For a fixed dimension k , a space $\mathbf{A}_{k,i}$ is discriminative for $f \in \mathcal{C}_i$ if the projection error of $S_J f$ in $\mathbf{A}_{k,i}$ is smaller than its projection in the other spaces $\mathbf{A}_{k,i'}$:

$$\forall i', \quad \|S_J f - P_{\mathbf{A}_{k,i'}}(S_J f)\|^2 \geq \|S_J f - P_{\mathbf{A}_{k,i}}(S_J f)\|^2,$$

with

$$\|S_J f - P_{\mathbf{A}_{k,i}}(S_J f)\|^2 = \|S_J f - \hat{\mu}_i\|^2 - \sum_{l=1}^k |\langle S_J f - \hat{\mu}_i, e_{i,l} \rangle|^2.$$

Model selection for classification is not about finding an accurate approximation model as in model selection for regression but looks for a discriminative model [2]. If $S_J f$ for $f \in \mathcal{C}_i$ is close to the class centroid $\hat{\mu}_i$ then low-dimensional affine spaces $\mathbf{A}_{k,i}$ are highly discriminative even if the remaining error is not negligible, because it is unlikely that any other low-dimensional affine space $\mathbf{A}_{k,i'}$ yields a comparable error. If f is an ‘‘outlier’’ which is far from the centroid $\hat{\mu}_i$ then a higher dimensional approximation space $\mathbf{A}_{k,i}$ is needed for discrimination. One can then adjust the dimensionality of the

discrimination space to each signal f by penalizing the dimension of the approximation space. The class index i of f is estimated by adjusting the dimension k of the space $\mathbf{A}_{k,i}$ that yields the best approximation, with a penalization proportional to the space dimension k [2]:

$$\hat{i}(f) = \underset{i \leq I}{\operatorname{argmin}} \min_{k \leq K} \|S_J f - P_{\mathbf{A}_{k,i}}(S_J f)\|^2 + \beta k.$$

This classification algorithm depends upon the penalization factor β and the scale 2^J of the scattering transform. These two parameters are optimized with a cross-validation mechanism. It minimizes a classification error computed on a validation subset of the training samples, which does not take part in the affine model learning.

- Increasing the scale 2^J reduces the intra-class variability of the representation by building invariance, but it can also reduce the distance across classes. The optimal size 2^J is thus a trade-off between both.
- The penalization parameter β is similar to a threshold on $|\langle S_J F - \hat{\mu}_i, e_{i,k} \rangle|^2$. The model increases the dimension k of the approximation space if the inner product is above β . Increasing β thus reduces the dimension of the affine model spaces, which is needed when the training sequence is small.

4. CLASSIFICATION RESULTS AND ANALYSIS

This section presents classification results for handwritten digit recognition, and for texture discrimination with illumination variations. The scattering transform is implemented with the same Gabor wavelets along $|\Gamma| = 6$ orientations for both problems, and the maximum scattering length is limited to $m_0 = 2$.

4.1. Handwritten Digit Recognition

The MNIST hand-written digit database provides a good example of classification with important deformations. Table 1 compares scattering classification results for training sets of variable size, with results obtained with deep-learning convolutional networks [12], which currently have the best results. Table 1 compares the PCA model selection algorithm applied on scattering coefficients and an SVM classifier with polynomial kernel whose degree was optimized, also applied on scattering coefficients. Cross validation finds an optimal scattering scale $J = 3$, which corresponds to translations and deformations of amplitude about $2^J = 8$ pixels, which is compatible with observed deformations on digits.

Below $5 \cdot 10^3$ training examples, a PCA scattering classifier provides state of the art results. It yields smaller errors than deep-learning convolution network which require large

Table 1. Percentage of error as a function of the training size for MNIST. Minimum errors are in bold. The last column gives the average model space dimension \bar{k} .

Training	ConvNets[12]	Scatt+SVM	Scatt+PCA
300	7.18	21.5	5.93
1000	3.21	3.06	2.38
2000	2.53	1.87	1.76
5000	1.52	1.54	1.27
10000	0.85	1.15	1.2
20000	0.76	0.92	0.9
40000	0.65	0.85	0.86
60000	0.53	0.7	0.74

training sets to optimize all network parameters with back-propagation algorithms. For 60 10^3 training samples, the deep-learning convolution network error [5] is below the scattering classifier error. Table 1 shows that applying a linear SVM classifier over the scattering transform degrades the results relatively to a PCA classifier up to large training sets, and it requires much more computations. This is an indirect validation of the linearization properties of the scattering transform.

Figure 1 shows the relative approximation error when approximating a signal class with an affine model in the scattering domain. For digits $i = 1$ and $i = 4$, it gives the average Intra-class approximation error of $S_J F_i$ with a space $\mathbf{A}_{k,i}$ of the same class, as a function of k :

$$\text{In}(i) = \frac{E\{\|S_J F_i - P_{\mathbf{A}_{k,i}} S_J F_i\|^2\}}{E\{\|S_J F_i\|^2\}}.$$

It is compared with

$$\text{Out}(i) = \frac{E\{\|S_J F_{i'} - P_{\mathbf{A}_{k,i}} S_J F_{i'}\|^2 \mid i \neq i'\}}{E\{\|S_J F_{i'}\|^2 \mid i \neq i'\}}.$$

which is the average Outer-class approximation error produced by the spaces $\mathbf{A}_{k,i}$ over all samples $S_J F_{i'}$ belonging to different classes $i' \neq i$. The intra-class error decay is much faster than the outer-class error decay for $k \leq 10$, which shows the discrimination ability of low dimensional affine spaces. For $k \geq 10$, intra-class versus outer-class distance ratio In/Out is approximatively 10^{-2} and 10^{-1} respectively for the digits $i = 1$ and $i = 4$. It shows the discrimination power of these affine models, and the much larger intra-class variability for hand-written digits 4 than for hand-written digits 1.

The US-Postal Service set is another handwritten digit dataset, with 7291 training samples and 2007 test images 16×16 pixels. The state of the art is obtained with tangent distance kernels [4]. Table 2 gives results with a PCA model selection on scattering coefficients and a polynomial kernel SVM classifier applied to scattering coefficients. The scattering scale was also set to $J = 3$ by cross-validation.

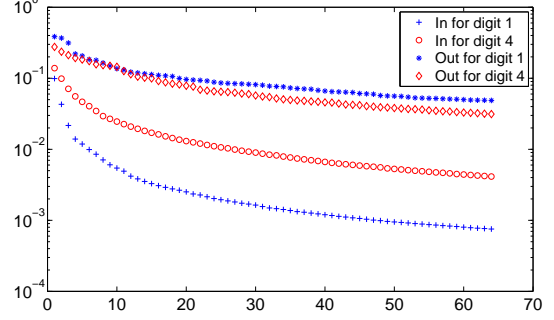


Fig. 1. Relative Intra-class In and average Outer-class Out approximation error for the digits $i = 1$ and $i = 4$.

Table 2. Error rate for the whole USPS database.

Scatt+PCA	Scatt+SVM	Tangent kern.[4]	humans
2.64	2.64	2.4	2.37

4.2. Texture classification: CUREt

The CureT texture database [7] includes 61 classes of image textures of $N = 200^2$ pixels, with 46 training samples and 46 testing samples in each class. Each texture class gives images of the same material with different pose and illumination conditions. Specularities, shadowing and surface normal variations make it challenging for classification. Figure 2 illustrates the large intra class variability, and also shows that the variability across classes is not always important.

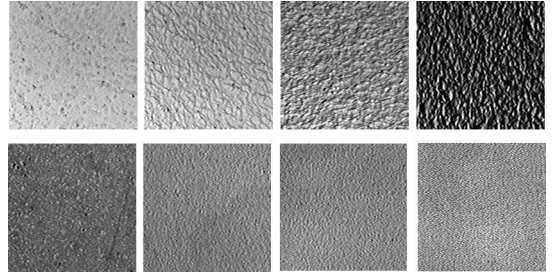


Fig. 2. Top row: images of the same texture material with different poses and illuminations. Bottom row: examples of textures that are in different classes despite their similarities.

Classification algorithms with optimized textons have an error rate of 5.35% [7] over this database, and the best result of 2.57% error rate was obtained in [13] with an optimized Markov Random Field model.

Wavelets have been shown to provide useful models for texture analysis [11]. Scattering classification results are shown in table 3, with exactly the same algorithm as for digit classification. With a PCA it greatly improves existing results with an error rate of 0.2%. The SVM classifier with an opti-

Table 3. Error rate for the CUREt database

Scatt+PCA	Scatt+SVM	Textons [7]	MRFs [13]
0.2 ± 0.08	1.71	5.35	2.57

mized polynomial kernel on scattering coefficients achieves a larger error rate of 1.71%.

The cross-validation adjusts the scattering scale $2^J = 2^7$ which is the maximum value. Indeed, these textures are fully stationary and increasing the scale reduces the variance of the scattering coefficients variability across realizations. Scattering vectors $S_J f$ at large scales 2^J have a small stochastic variability within each texture class because of the averaging by ϕ_J . Moreover, global invariance to rotation and illumination changes is provided by the PCA classification algorithm. These invariant linear space models are learnt effectively even with few training samples. This example shows that linear models are a simple yet powerful mechanism to generate invariance for classification problems.

5. CONCLUSION

As a result of their translation invariance and Lipschitz regularity to deformations, scattering operators provide appropriate representations to model complex signal classes with affine spaces calculated with a PCA. Classification with model selection provides state of the art results with limited training size sequences, for handwritten digit recognition and textures. As opposed to discriminative classifiers such as SVM and deep-learning convolution networks, these algorithms learn a model for each class independently from the others, which leads to fast learning algorithms.

Scattering operators can be defined on more general Lie groups other than the group of translations, such as the group of rotations or scaling [10]. The intra-class variability due to the action of several transformation groups can be contracted by combining scattering operators adapted to each of these groups [10]. On signal classes including clutter and more complex variability, one can estimate the deformation group responsible of most of the intra-class variability, provided one has enough training samples.

6. REFERENCES

- [1] R.Basri, D.Jacobs : “Lambertian Reflectance and Linear Subspaces”, IEEE transactions on Pattern Analysis and Machine Intelligence, feb 2003.
- [2] G. Bouchard and G. Celeux “Selection of generative models in Classification”, IEEE Trans on PAMI,28, 544-554, (2006).
- [3] J. Bouvrie, L. Rosasco, T. Poggio: “On Invariance in Hierarchical Models”. NIPS 2009.
- [4] B.Haasdonk, D.Keysers: “Tangent Distance kernels for support vector machines”, 2002.
- [5] K. Jarrett, K. Kavukcuoglu, M. Ranzato and Y. LeCun: “What is the Best Multi-Stage Architecture for Object Recognition?”, Proc. International Conference on Computer Vision (ICCV’09), IEEE, 2009.
- [6] Y. LeCun, K. Kavukcuoglu and C. Farabet: “Convolutional Networks and Applications in Vision”, Proc. International Symposium on Circuits and Systems (ISCAS’10), IEEE, 2010
- [7] T. Leung, and J. Malik; “Representing and Recognizing the Visual Appearance of Materials Using Three-Dimensional Textons”. International Journal of Computer Vision, 43(1), 29-44; 2001.
- [8] W. Lohmiller and J.J.E. Slotine “On Contraction Analysis for Nonlinear Systems”, Automatica, 34(6), 1998.
- [9] S. Mallat. “Recursive Interferometric Representation”, Proc. of EUSICO conference, Denmark, August 2010.
- [10] S. Mallat. “Group Invariant Scattering”, CMAP Technical Report, 2010.
- [11] J. Portilla and E P Simoncelli, “A Parametric Texture Model based on Joint Statistics of Complex Wavelet Coefficients”, Int. Journal of Computer Vision, 40(1):49-71, October, 2000
- [12] M. Ranzato, F.Huang, Y.Boreau, Y. LeCun: “Unsupervised Learning of Invariant Feature Hierarchies with Applications to Object Recognition”, CVPR 2007.
- [13] M.Varma, A. Zisserman: “A Statistical Approach To Material Classification Using Image Patch Exemplars”. IEEE Transactions on Pattern Analysis and Machine Intelligence , 31(11):2032–2047, November 2009.
- [14] R.Vershynin: “How close is the sample covariance matrix to the actual covariance matrix?”, Apr 2010